Version 1.1, Jul 2003

Application Note

AN-EMI-01

Considerations of conducted EMI in SMPS

Author: Jenny Pirwitz
Ilia Zverev

Published by Infineon Technologies AG

http://www.infineon.com

Power Management & Supply

Never stop thinking.

1. Abstract

This application note discusses the aspects of ElectroMagnetic Interference (EMI) emission in switch-mode power supplies (SMPS). A short overview of the active regulations in selected regions and an example of the measurement of conducted EMI will be given. Several MOSFET related factors influential on the EMI in SMPS will be investigated experimentally. Different operating modes of a flyback converter (hard switching and quasi resonant) will be discussed regarding their influence on the electrical noise generation. General design guidelines will be given.

2. Basics of EMI

ElectroMagnetic Compatibility (EMC) is the ability of an electrical installation to work properly in an electromagnetically polluted environment as well as not to disturb other electrical devices due to the emission oft electromagnetic interferences. It means that the electrical devices don't influence themselves and one another, e.g. via the common ground of control- and power circuits.

Electromagnetic interference is generated by a varying electric or magnetic field. It is transmitted by means of conductive, inductive or capacitive coupling, through free space or a combination of these means. It can be measured as conducted or radiated interferences. This application note will focus mainly on conducted interference.

Conducted interferences can be distinguished into asymmetrical and symmetrical interferences, common and differential mode respectively. The differential mode current only flows at the connecting line. The common mode circuit is closed across parasitic capacitors C_p to the earth ground and the connecting lines. The interference sink can be the main or another device connected with the source. Fig. 1 shows both phenomena.

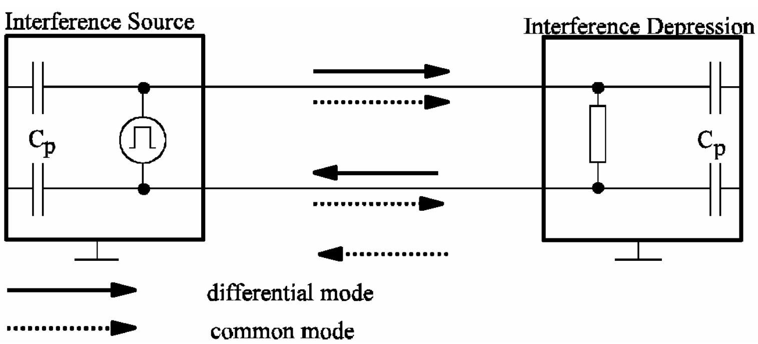

Fig. 1 Conducted interference mechanism

Periodical rectangle functions in time domain generate a discrete line spectrum decreasing with 20 dB per decade in the frequency domain. The spectral lines are multiples of the basic frequency (Fig. 2 a and c).

Real waveforms of power switch cycles with turn on (τ_r) and turn off times (τ_f) are trapezoidal.

Fourier transformation converts the waveforms from time domain in to the frequency domain or spectrum. The frequency domain for a trapezoidal waveform can be characterized by spectrum envelope (Fig. 2 b and d).

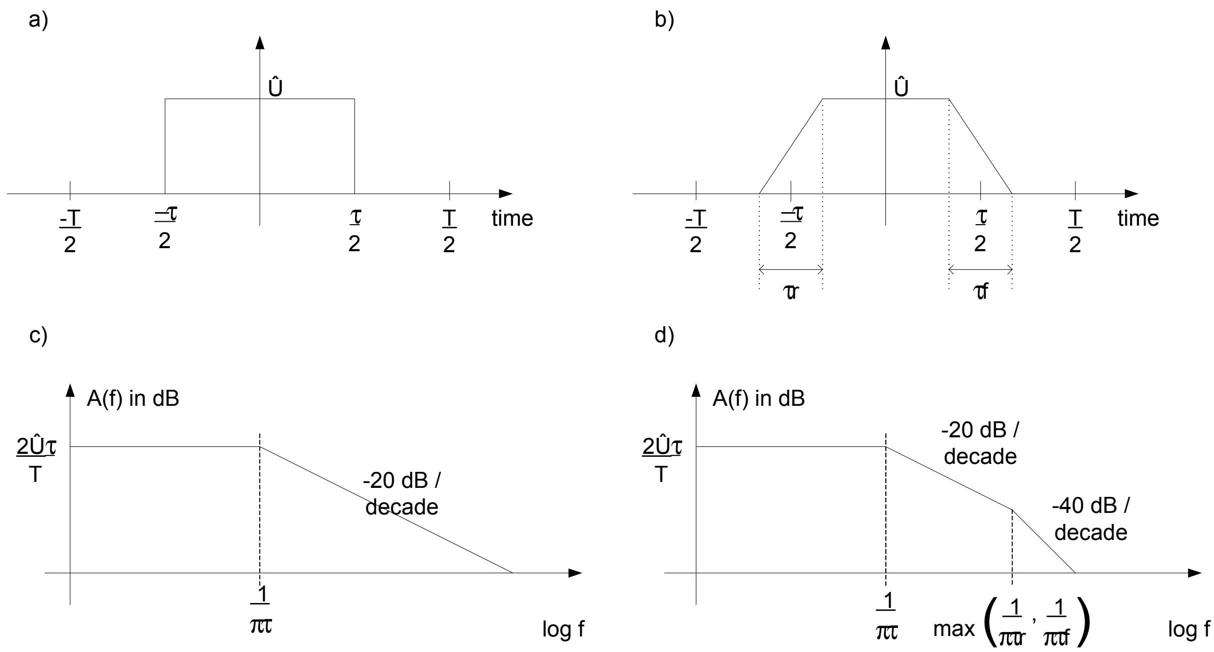

Fig. 2 Ideal rectangle and trapezoidal functions in time (a, b) and frequency domain (c, d)

The first sharp bend in the spectrum is determined by the pulse width τ and can be calculated as shown in Fig. 2. Starting at this frequency the spectrum decreases with 20 dB per decade. With τ_r equal τ_f the spectrum will decrease starting at this frequency with - 40 dB per decade. Otherwise the second sharp bend is determined by the faster slope, either τ_r or τ_f.

3. EMI regulations

A wide range of regulations regarding EMI exists in different countries. This application note gives a short overview of the major ones. The intention is it to give a reference to the international standard (CISPR).

3.1. USA

The EMI regulations are specified in Title 47 of the “Code of Federal Regulations” in chapter 1 “Federal Communications Commission”. Part 15 treats the “Radio frequency devices”[1] and part 18 the “Industrial, scientific, and medical equipment (ISM)”[2]. In Fig. 3 the limit value for the radio interference voltage is represented according to part 15 and 18.

[1] http://www.access.gpo.gov/nara/cfr/waisidx_02/47cfr15_02.html
[2] http://www.access.gpo.gov/nara/cfr/waisidx_02/47cfr18_02.html

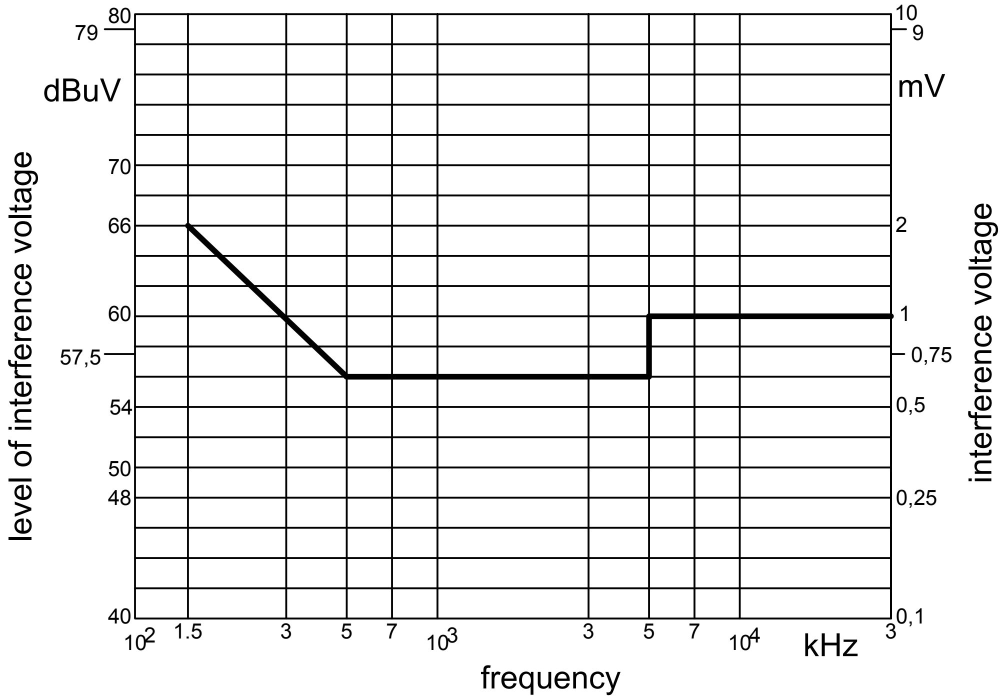

Fig. 3 Limits for the radio interference voltage (Quasi-peak)

3.2. Japan

In Japan the EMI suppression of information-technical installations is voluntary. The requirements for the VCCI Mark correspond to the CISPR 22. A condition for the use of the VCCI Mark is the membership in the VCCI (Voluntary Control Council for Interference) and the testing in a listed EMI laboratory.

The Mutual Recognition Agreement between Europe and Japan [3] contains the Electrical Appliance and Material Safety Law [4] on Japanese side, which doesn't include EMI requirements and on European side the low-voltage- and EMI regulation.

3.3. Taiwan

In Taiwan since 1 June 2000 exits the new certification system "Registration of Product Certification (RPC)". The product requirements correspond to the international standards, like listed in Tab. 1.

CNS	CISPR
13783-1	14-1
14115	15
13438	22
13439	13
13803	11

Tab. 1 Analogy of Taiwan and international regulations

Additional details are published in the web at the "Bureau of Standards, Metrology and Inspection" in the EMC regulations[5].

[3] http://www.soumu.go.jp/joho_tsusin/eng/Resources/laws/MRA_Law_final.pdf
[4] http://www.jetro.go.jp/se/e/standards_regulation/denan-2001nov-e.pdf
[5] http://web-server.bsmi.gov.tw/english/emc/e_emc_hp.htm

3.4. China

In China on 1 May 2002 was established a new certification system “The Compulsory Product Certification System” by the China National Regulatory Commission for Certification and Accreditation (CNCA). All in the “First Catalogue of Products Subject to Compulsory Certification” listed products, have to be accredited by a center, which is approved by the CNCA, in order to receive the CCC-Mark.

In this catalogue the EMI is not mentioned, however the product specific requirements include EMI regulations; i.e. “Low-voltage Electrical Apparatus - switch and control Equipment” and “Electric Tools”. Few of them have references to the Chinese standards like GB4343-1995.

3.5. Hong Kong

In Hong Kong the requirements refer only to emission and are specified in the Chapter 106B of “Telecommunications (Control of Interference) Regulations”. The limits of the interference voltage are similarly the CISPR 22, but in the law explicitly defined.

3.6. Europe

The European standards correspond as showed in Tab. 2 to the international ones.

product	European Standard EN	International Standard
electrical motor-operates & thermal appliances, electric tools & similar apparatus	55014	CISPR 14
electrical lighting and similar equipment	55015	CISPR 15
TV receivers and audio equipment	55013	CISPR 13
Information Technology	55022	CISPR 22
ISM equipment	55011	CISPR 11

Tab. 2 Analogy of European and International standards

4. Measurement of interference voltage (according to VDE 0876/77)

The details of the measurement setup and methods are described in the different EMI regulations; however the majority of them follow a similar principle. Practical experience teaches that it will be beneficial to introduce an additional safety margin of 3 to 6 dB below the norm limit line in order to avoid possible tolerances during the manufacturing, aging effects, etc.

4.1. Measurement setup

The measurement of the radio interference voltage is made with a help of a line impedance stabilization network (LISN). This stabilization network ensures a constant and reproducible main line impedance for the test object (DUT), the coupling of the interference signal to the radio interference meter and a blocking of conducted interferences from and into the main line.

In the next part only the most important requirements will be represented. For further details, like cable length and placement, please refer to the regulations.

The test object is placed on a table of non conductive material at least 80 cm high in a distance of 40 cm to a grounded, conducting wall of metal of at least 2 x 2 m² surface. Moreover a distance of at least 80 cm to other grounded metal surfaces is to be kept. Fig. 4 shows the basic configuration according to these requirements.

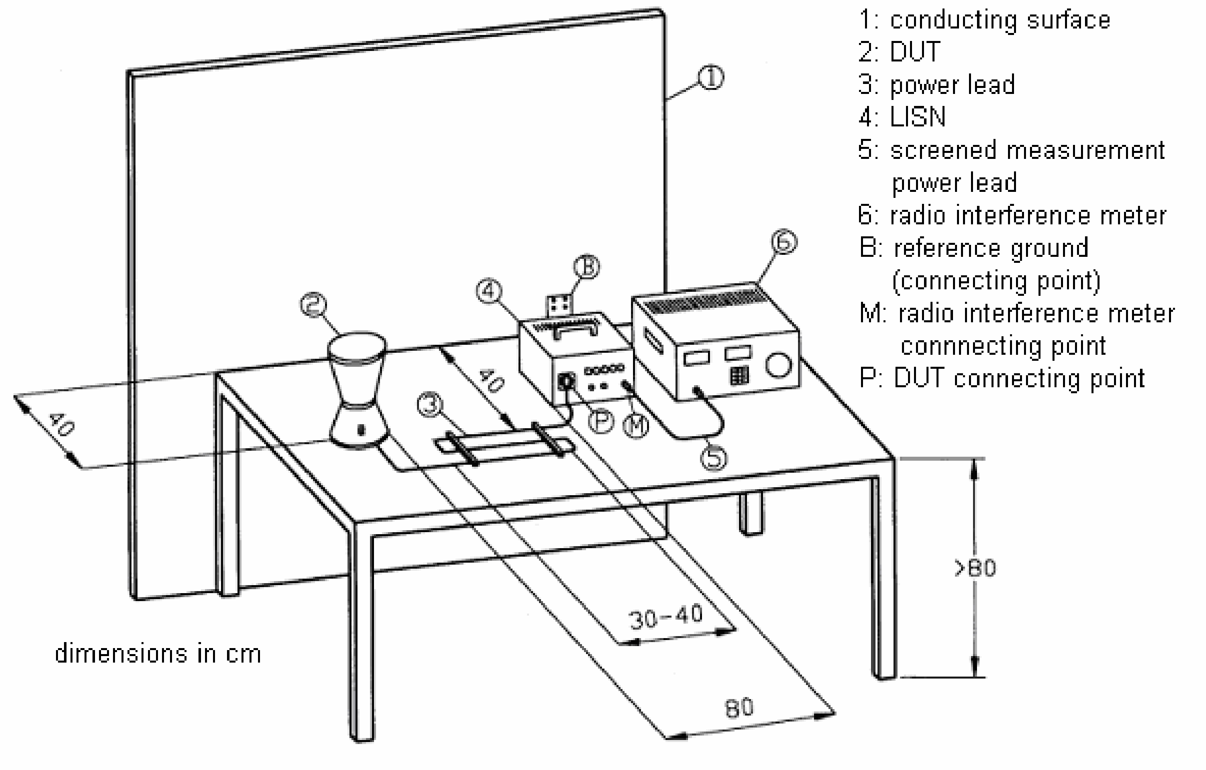

Fig. 4 Measurement setup according to VDE 0877/CISPR 16-2

4.2. Measurement methods

For the different measuring procedures the radio interference meter is equipped with different measuring rectifiers. The 6 dB-bandwidth range is varying for the different frequencies, as it can be seen in Tab. 3.

6 dB-bandwidth	frequency range
200 Hz	10 to 150 kHz
9 kHz	150 kHz to 30 MHz
120 kHz	30 MHz to 1,2 GHz

Tab. 3 Main parameter of the radio interference meter

Fig. 5 demonstrates the limit values for the radio interference voltage according to VDE 0876 part 1a.

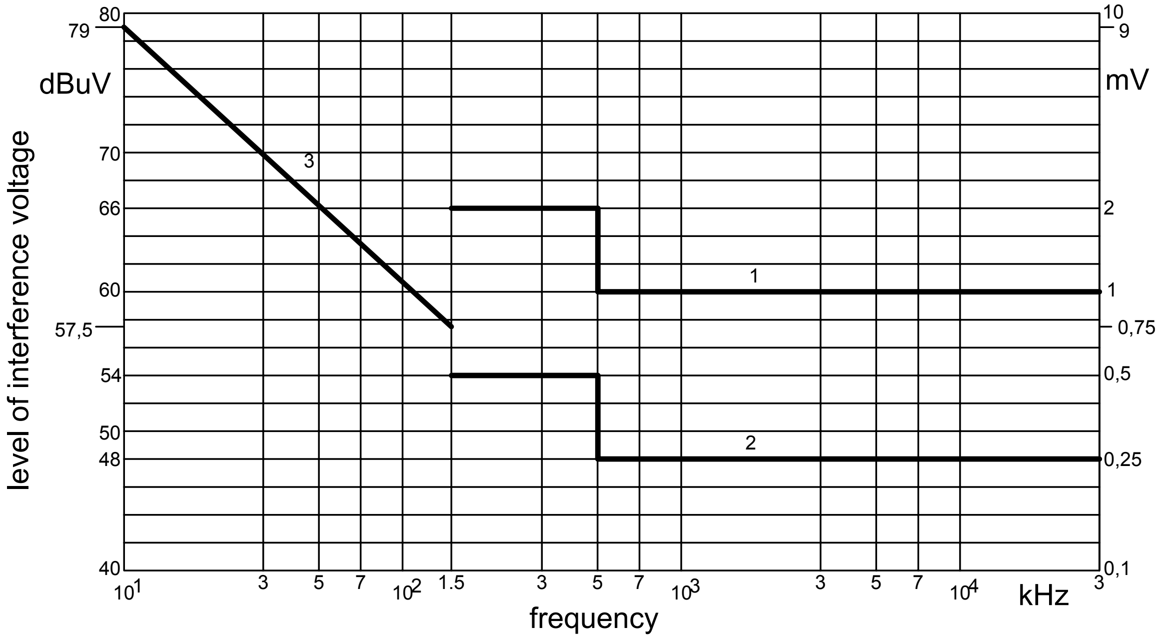

1 Limits for radio interference voltage with wideband frequency spectrum in the frequency range from 150 kHz to 30 MHz

2 Limits for spectral component appearing on discrete frequencies in the frequency range from 150 kHz to 30 MHz

3 Limits for radio interference voltage in the frequency range from 10 to 150 kHz (recommended)

Fig. 5 Limits for the radio interference voltage (according to VDE 0876 part 1a)

The regulation contains different types of measurements – peak, quasi peak and average detection.

4.2.1. Peak detection

During the peak detection the highest instantaneous value of the voltage is measured within a fixed observation time. For the registration of the peak value the detector must have a fast rise, thus a small time constant, and a very slow fall, respective a large time constant. After reaching the maximum the measured value remains almost constant and independent of further variations or following frequencies of the measured variable. The peak detection is the simplest and fastest method to measure conducted emission with small cycle times. Fig. 6 shows the evaluation detector for the peak detection.

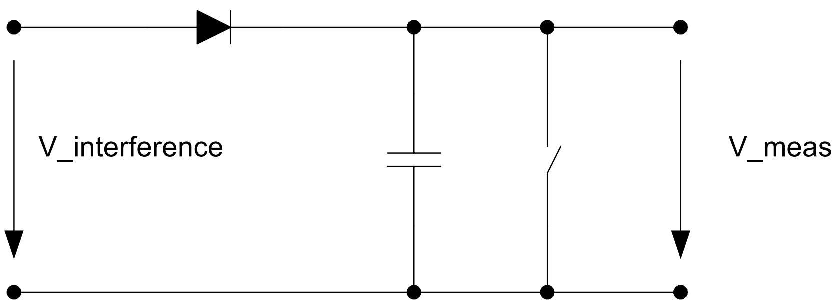

Fig. 6 Evaluation detector for peak detection

4.2.2. Quasi-Peak detection

The measured peaks are evaluated according to their frequency. The evaluation considers the physiological impression of disturbances, which are caused by successive impulses. Specifications for the evaluation are given in VDE 0876 part 1/9.78.
A Quasi-peak detector behaves like a peak detector with a shorter discharging time constant (Fig. 7).

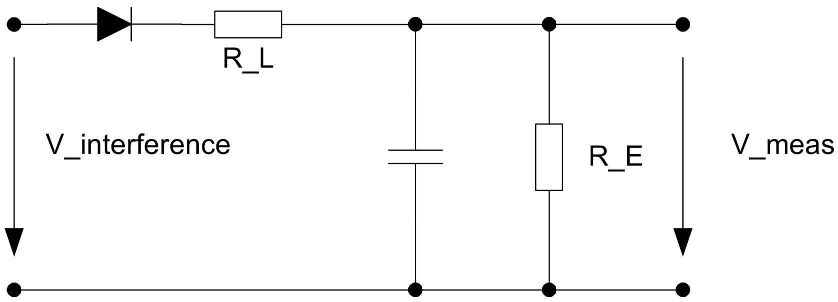

Fig. 7 Evaluation detector for quasi-peak detection

4.2.3. Average detection

The average detector is a low-pass filter with the cut-off frequency significant lower than the pulse frequency. It's used for the measurement of interferences on discrete frequencies. The average detector (Fig. 8) is insensitive to glitches and modulating frequencies.

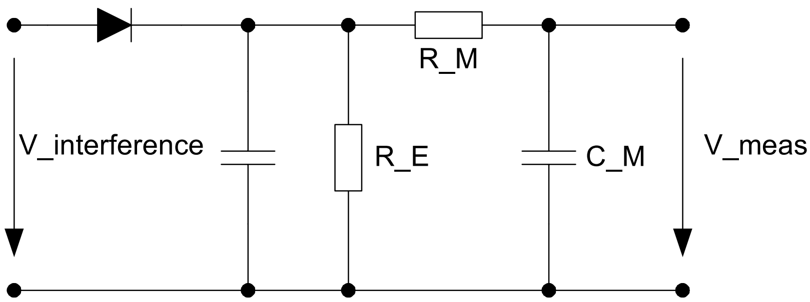

Fig. 8 Evaluation detector for average detection

5. EMI in Switched Mode Power Supplies (SMPS)

Switched Mode Power Supplies are usually a part of a complex electronic system. The system operates with electric signals with much lower amplitude and energy compared to those on an SMPS. It means that usually the SMPS is the strongest electrical noise generator in the whole system.
Especially the power switches with their high *dv/dt* and *di/dt* switching slopes are the sources of EMI. The source of differential mode interferences is the current switched by a MOSFET or a diode. High rates of *dv/dt* and parasitic capacitors to the ground are the reasons for common mode interferences.

5.1. Factors of influence on EMI spectrum

Different parameter can affect the EMI spectrum of an SMPS, e.g. the switching slopes of the power semiconductors, the operating point regarding switch voltages and currents. Some of these influence factors will be analyzed in this chapter.

5.1.1. Test setup

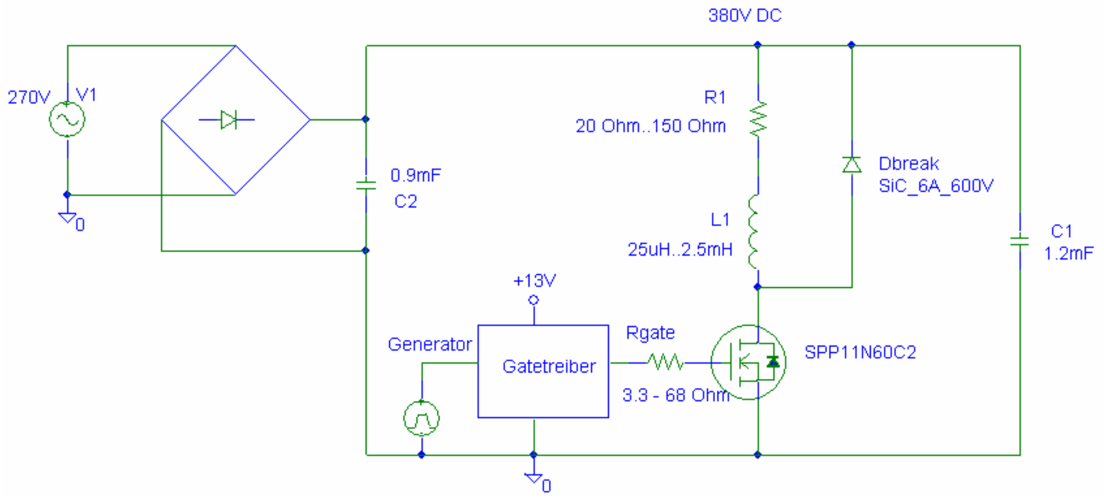

Fig. 9 Test chopper

The results presented in this chapter have been made using the shown test setup (Fig. 9), if not other specified. The test setup is a chopper without an EMI filter using 380mΩ/11A/600V CoolMOS™ and thinQ!™ Silicon Carbide Schottky diode. It can be operated in Discontinuous and Continuous Conduction Modes.

5.1.2. External gate resistance

The well-known way to control the switching speed and therefore the EMI behavior is a variation of the external gate resistance. If the resistance will be increased, the time constant determined by this resistance and the capacitance of the MOSFET will be increased as well. The switching transient will be slowed down and thereby the electrical noise becomes lower. Fig. 10 shows the controllability of the *di/dt* and *dv/dt* values for turn on and turn off transients of CoolMOS™ SPP11N60C3.

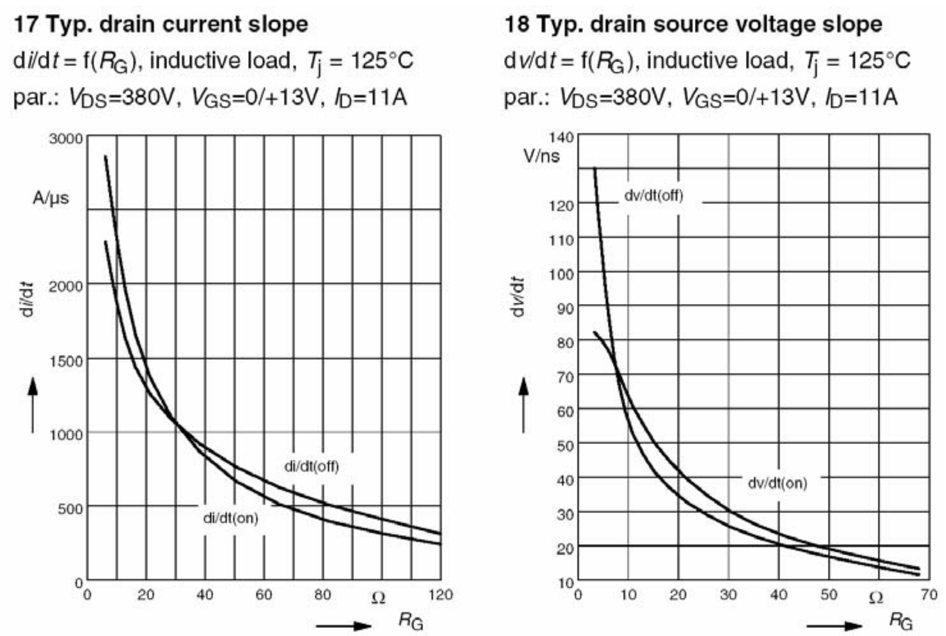

Fig. 10 Typical switching slopes versed gate resistance of CoolMOS™ SPP11N60C3 (datasheet information)

As it can be seen the drain current and drain to source voltage slopes can be adjusted simply using the external gate resistor during turn on and off transients. The noise emission can be also controlled in this way in high frequency range (Fig. 11 and Fig. 12).

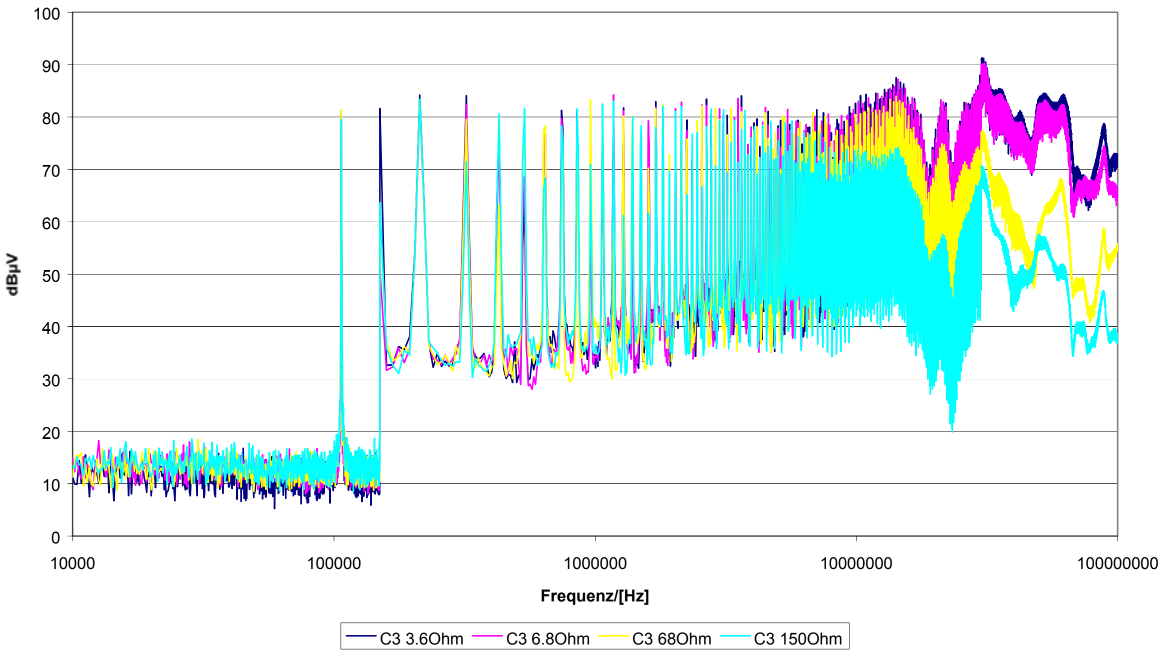

Fig. 11 Influence of the external gate resistance (discontinuous current mode, Id=6A, measured)

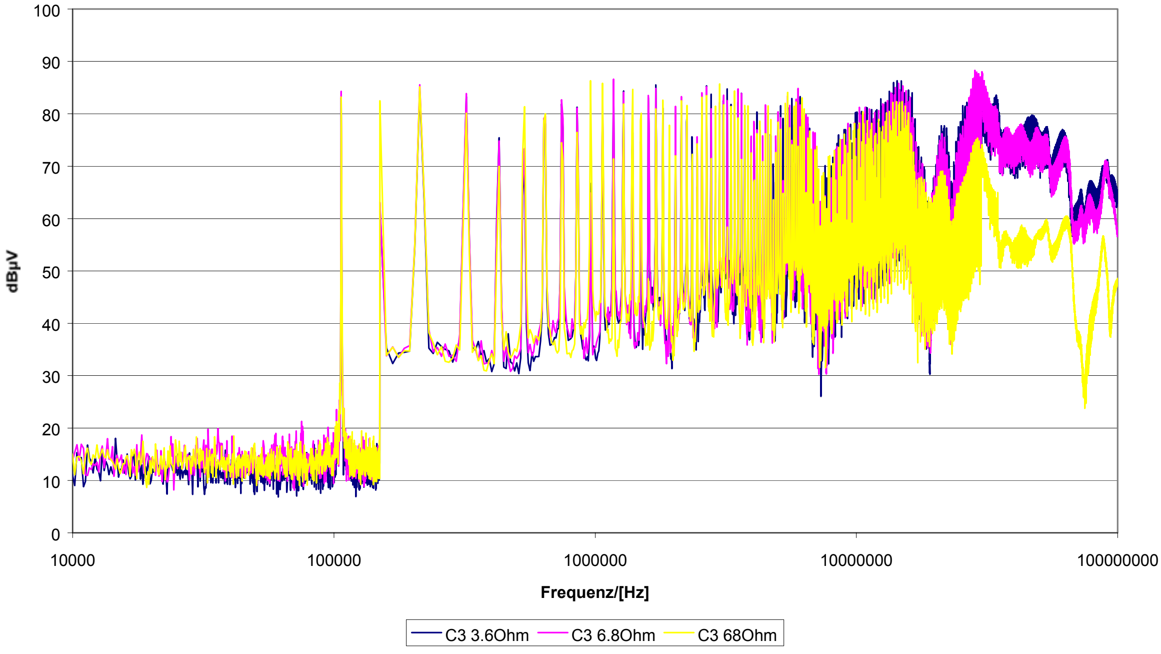

Fig. 12 Influence of the external gate resistance (continuous current mode, Id=6A, measured)

5.1.3. Gate-source and drain-source voltage

The appropriate spectrum for 6 A peak drain-current, 13 V gate voltage and 380 V drain-source voltage has been chosen as reference.
Different maximum values of the gate-source voltage (or V_{cc} of the control IC) were investigated – 10V, 13V and 15V.
Also the variation of the bus voltage from 380V to 200V has been measured.

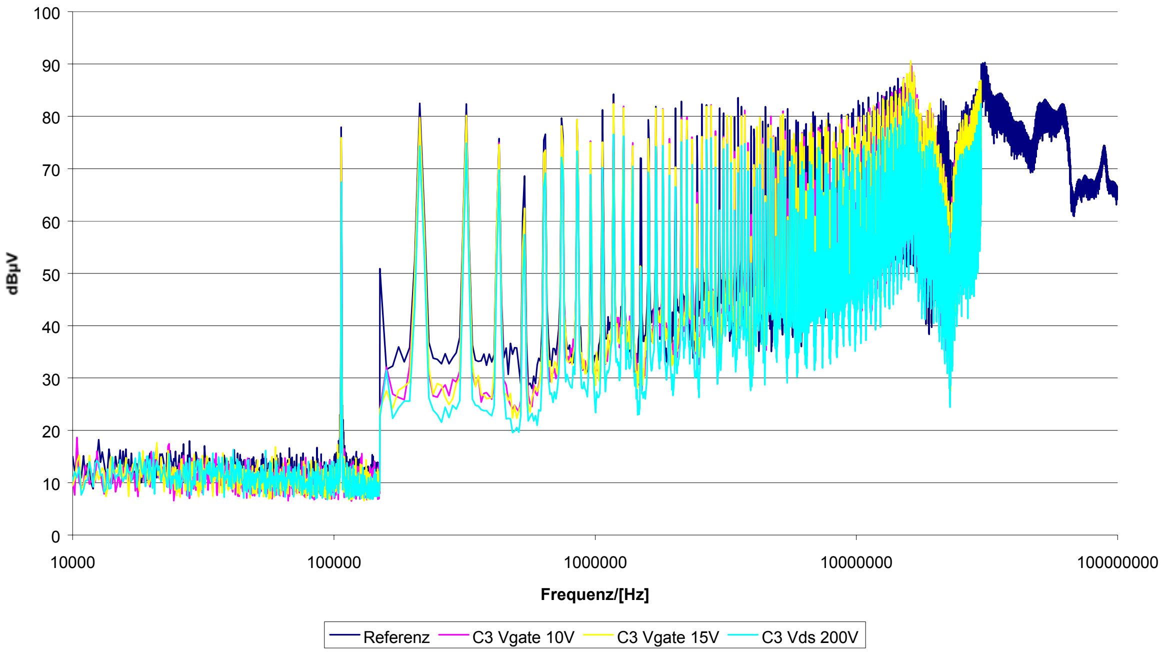

Fig. 13 Influence of the gate and drain-source voltage (discontinuous conduction mode, Id=6A, Rgate=6.8 Ohm, measured)

Fig. 13 shows that a change of the gate voltage from 10V to 15V hardly influences the spectrum. It can be explained by the fact, that 10V is still high enough to fully open the MOSFETs channel. Further reduction to values close to Miller plateau for the given operating point will slow down the switching and reduce the spectra.
The decrease of the drain-source voltage or bus voltage affects the entire spectrum evenly according to Fourier theory. It means that the spectrum will decrease with the gate voltage.

5.1.4. Drain current

The peak values of the drain current have been varied in discontinuous (2A, 6A, 11A) and continuous (2A, 6A) conduction modes.

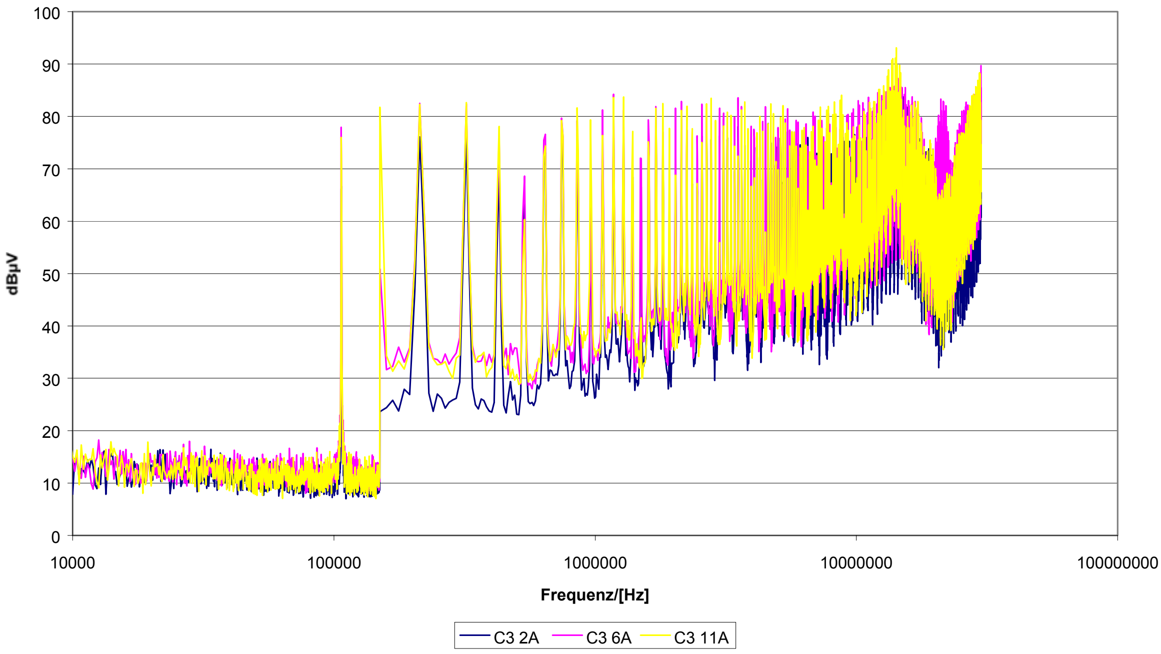

Fig. 14 Influence of the drain current (discontinuous current mode, Rgate=6.8 Ohm, measured)

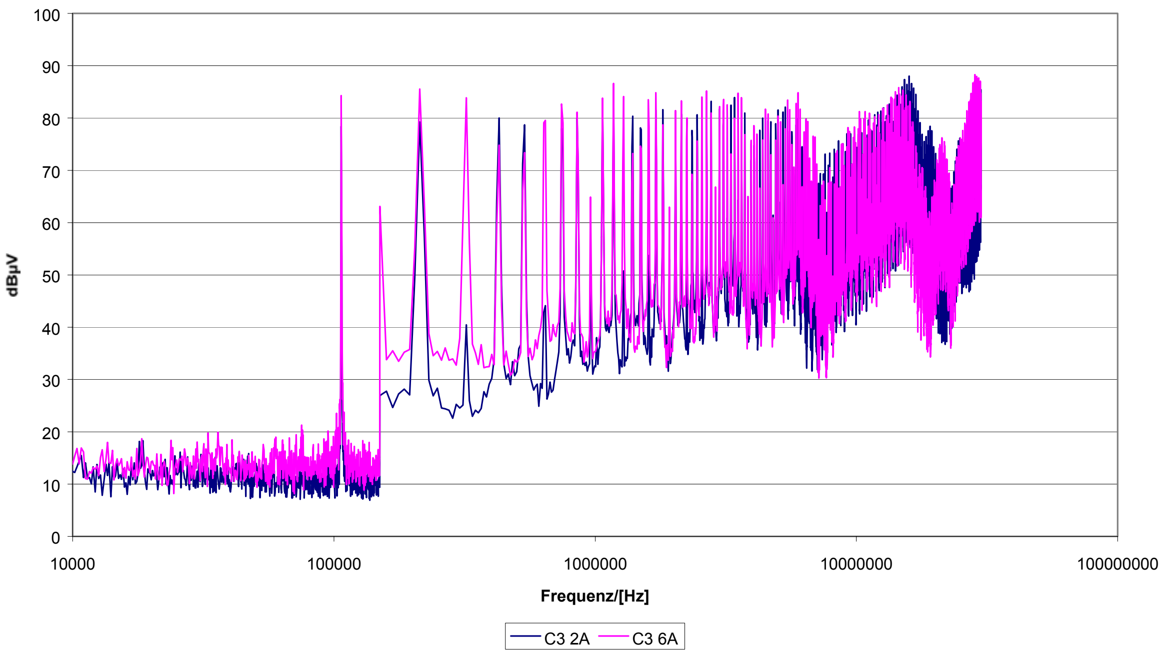

Fig. 15 Influence of the drain current (continuous conduction mode, Rgate=6.8 Ohm, measured)

Only little differences in the frequency range under 1 MHz at different current peak values (Fig. 14 and Fig. 15) can be noticed except from some resonance frequencies. The drain current was not decreased enough to operate the CoolMOS™ switch in the linear field of its output characteristic. Thus the *dv/dt* of the switch remained the same and thereby the spectrum changes can be hardly recognized.

5.2. Flyback converter example

5.2.1. Analysis of basic waveforms

The analysis of the basic waveforms will be done on a simulated example of a flyback converter operating in discontinuous conduction mode. Typical drain-source voltage waveform of the primary side switch is shown in Fig. 16.

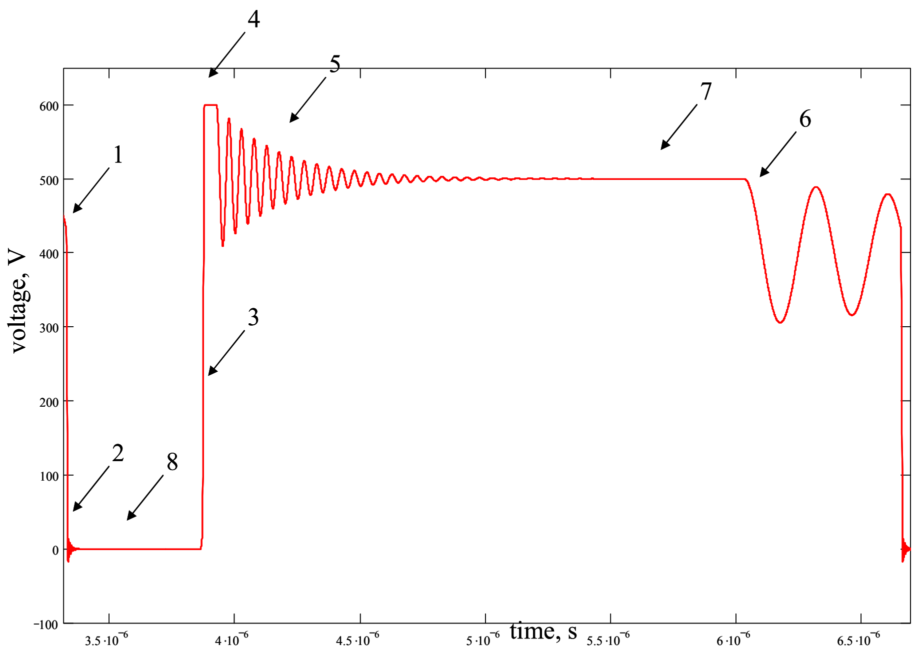

Fig. 16 Typical drain-source voltage of the MOSFET in a flyback

These drain-source voltage waveforms can be theoretically distinguished into typical elements. Different physical phenomena influence the waveform at given time interval. Fig. 17 and Tab. 4 demonstrate the main elements of the voltage waveform. The superposition of all these elements results in a typical drain-source voltage shown in Fig. 16.

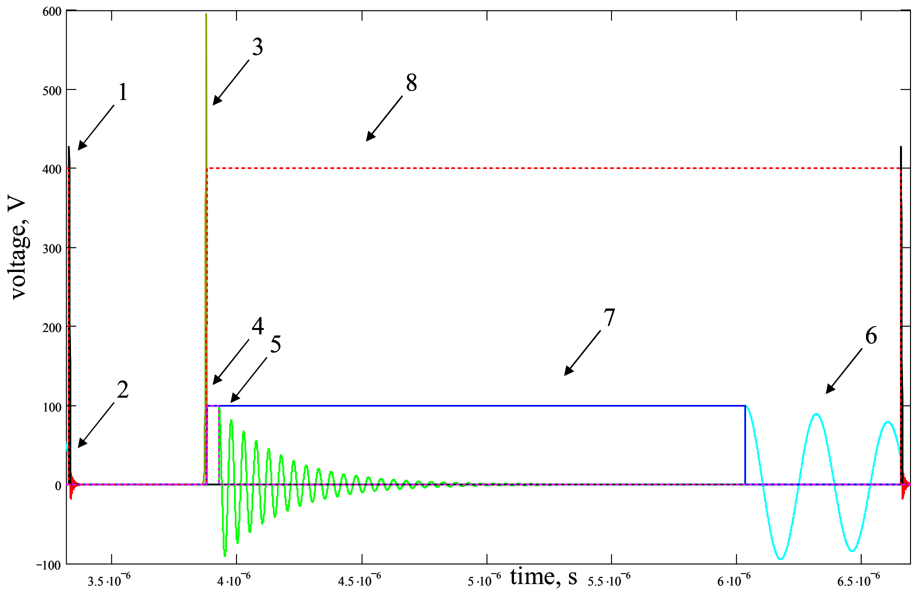

Fig. 17 Main elements of the drain-source voltage

<table>
<tr>
<td>Element 1:
voltage fall during turning on
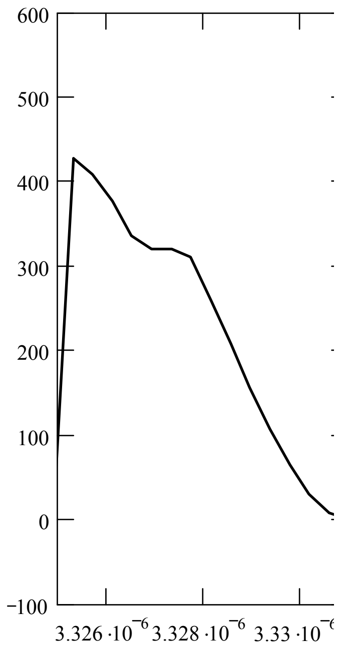</td>
<td>Element 2:
parasitic oscillation during turning on due to current spike
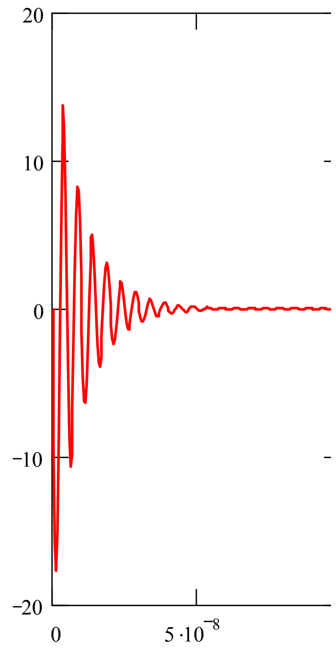</td>
<td>Element 3:
voltage rise during turning off
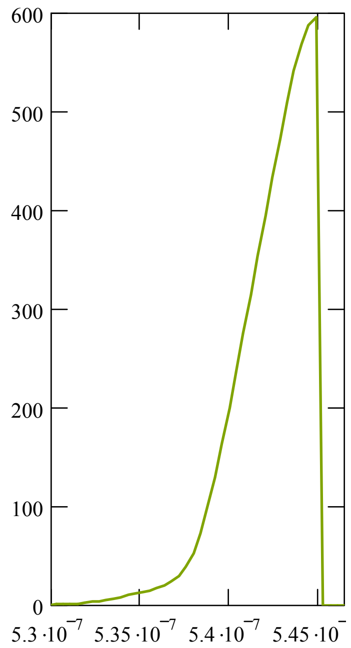</td>
</tr>
<tr>
<td>Element 4:
clamping voltage of snubber
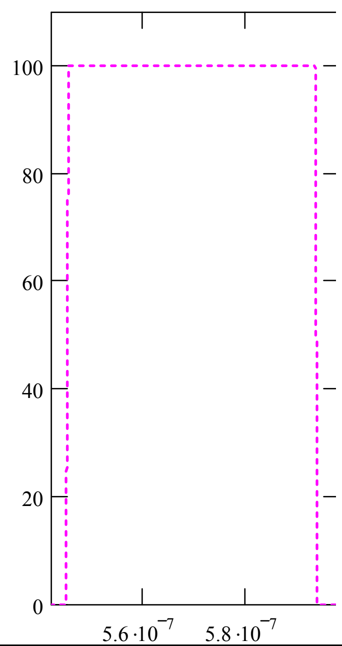</td>
<td>Element 5:
parasitic oscillation after clamping involving mainly the output capacitance of the MOSFET and the leakage inductance of the transformer
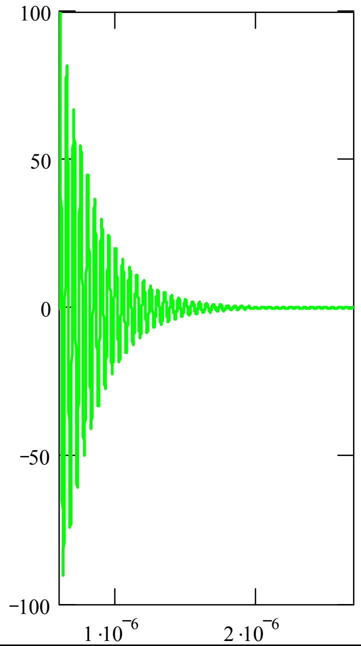</td>
<td>Element 6:
parasitic oscillation after flyback phase involving mainly the output capacitance of the MOSFET and the magnetization inductance of the transformer
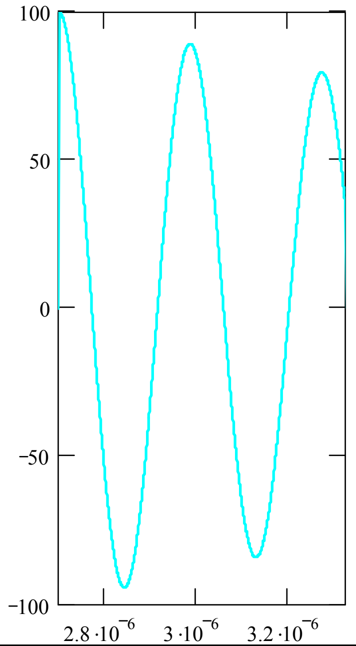</td>
</tr>
</table>

Tab. 4 Main elements of the drain-source voltage

Element 7:
reflected voltage during the flyback phase
Element 8:
main rectangular signal with bus amplitude

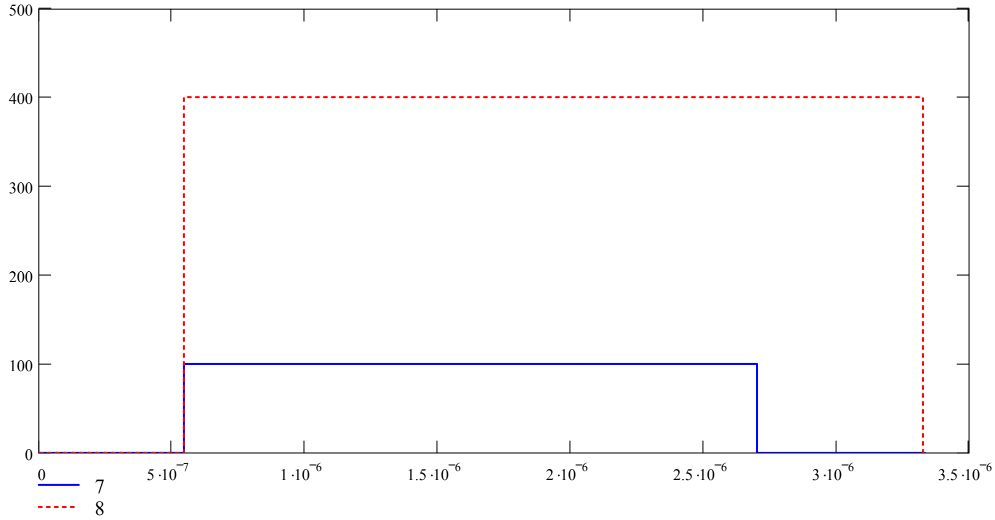

Tab. 4 Main elements of the drain-source voltage (continued)

The spectrum of the whole drain-source waveform (Fig. 16) is presented in Fig. 18.

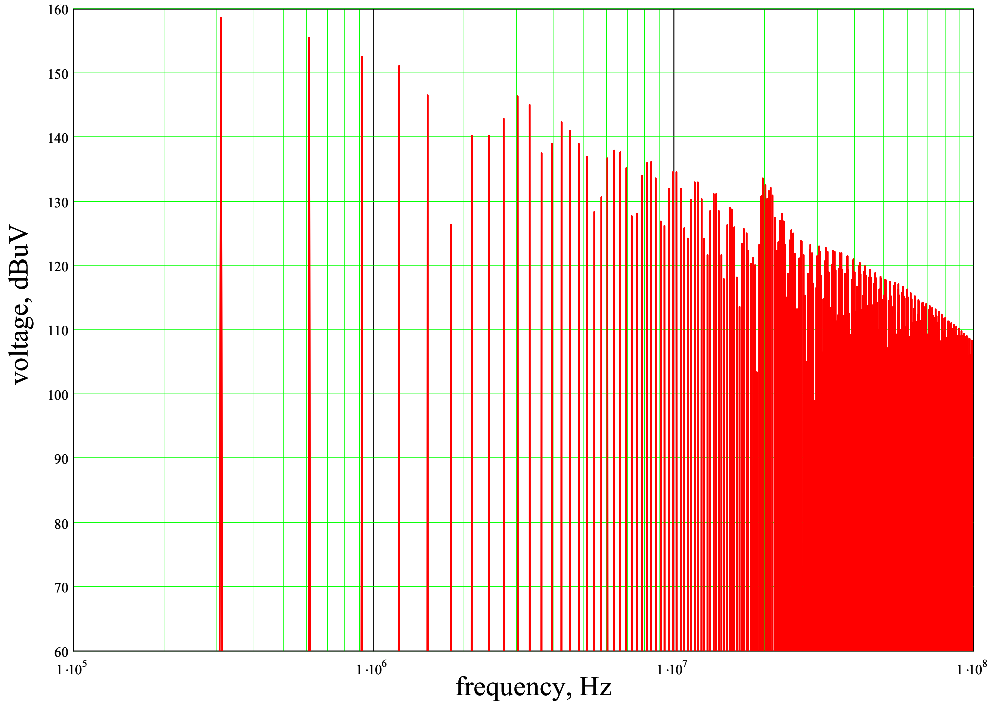

Fig. 18 Spectrum of the drain-source voltage (as shown in Fig. 16)

The spectra of the main elements of the drain-source voltage can be found in Fig. 20. Fig. 19 is exactly the same as Fig. 17 and has been repeated here for better understanding.

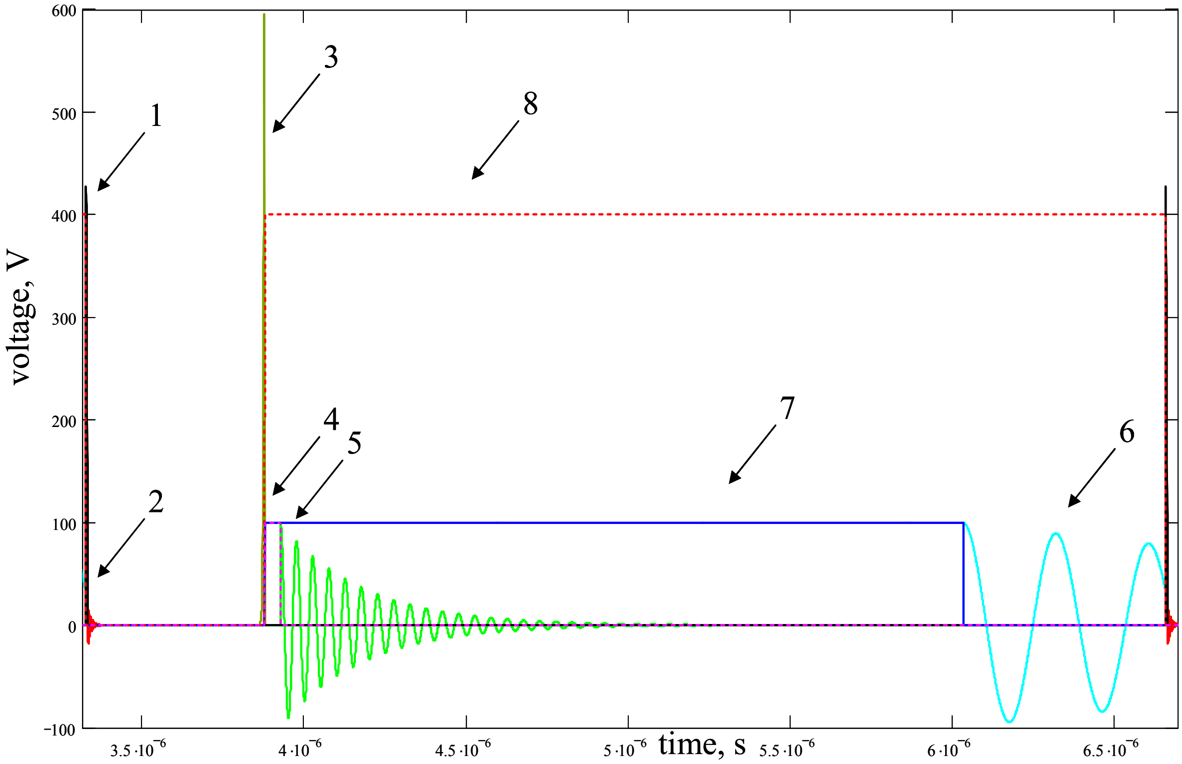

Fig. 19 Main elements of the drain-source voltage (repeated, same as Fig. 17)

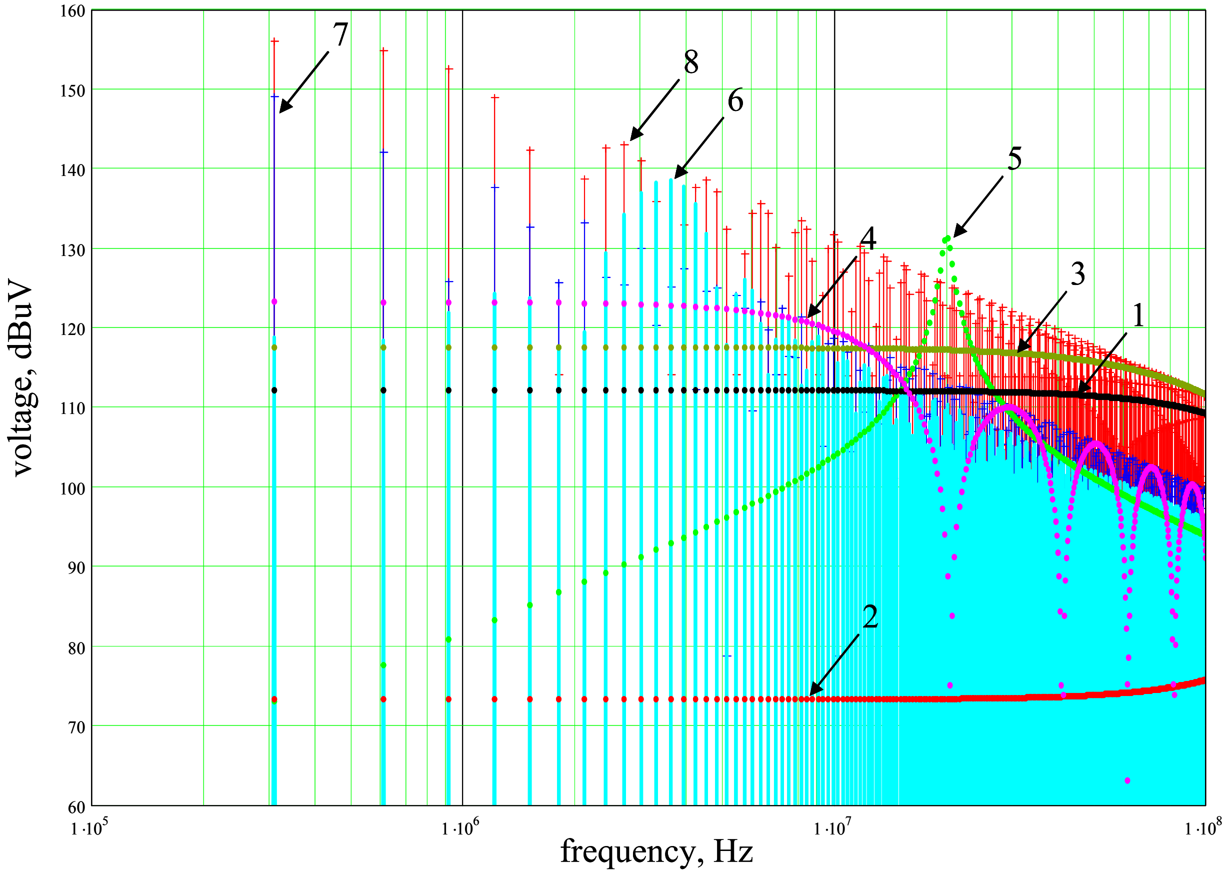

Fig. 20 Spectra of the main elements of the drain-source voltage

This method allows associating certain parts of the spectrum with their root causes, i.e. the peak at 20 MHz in the spectrum of the drain-source voltage is caused by the parasitic oscillation due to the output capacitance of the MOSFET and the leakage inductance of the transformer.

The analysis of the drain current of the primary switch will be done in the same way. Fig. 21 demonstrates a typical drain current in a DCM flyback.

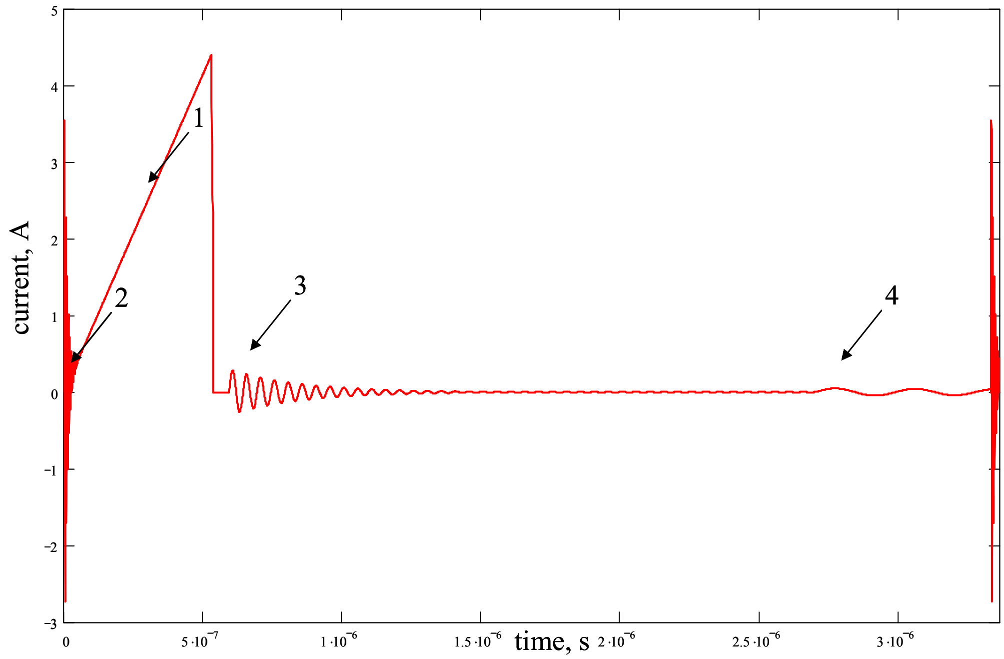

Fig. 21 Typical drain current in a flyback

This waveform can be presented as a superposition of the following elements (Fig. 22 and Tab. 5). The superposition of all these elements results in a typical drain current shown in Fig. 21.

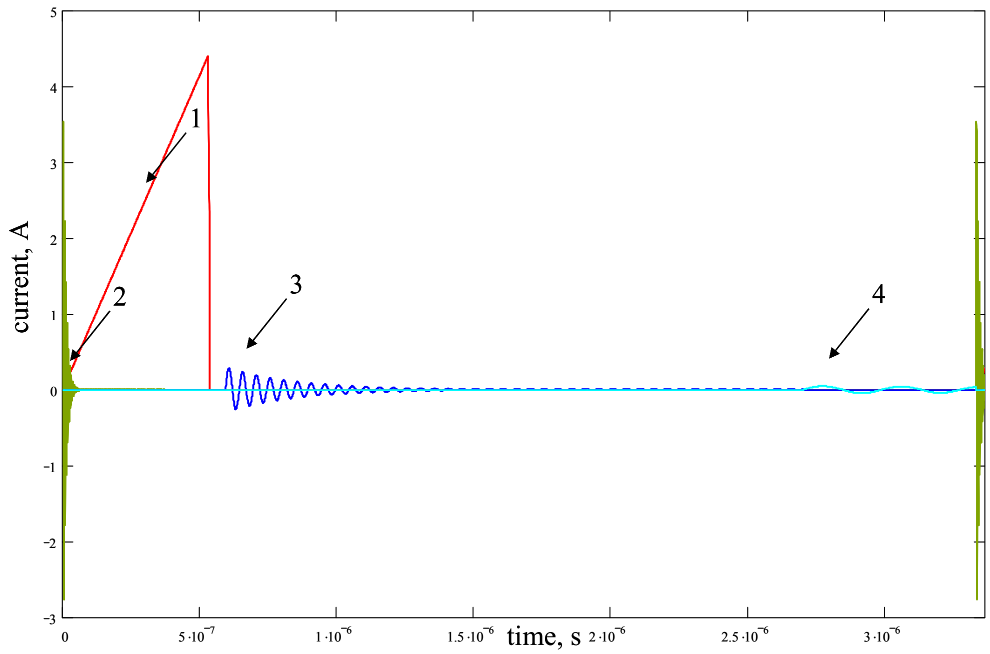

Fig. 22 Main elements of the drain current

<table>
<tr><td colspan="3">Element 1:
main triangle of the drain current</td></tr>
<tr><td colspan="3">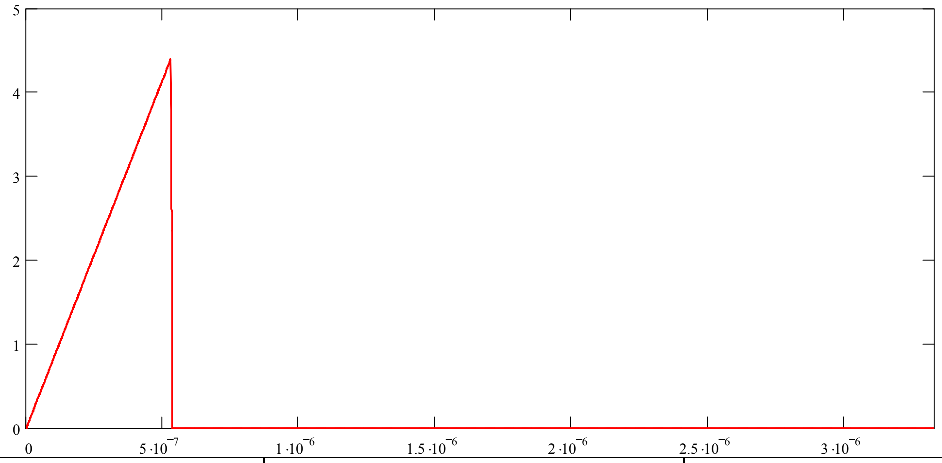
</td></tr>
<tr><td>Element 2:
current spike during turning on due to parasitic capacitances of the circuit</td><td>Element 3:
parasitic oscillation after clamping involving mainly the output capacitance of the MOSFET and the leakage inductance of the transformer</td><td>Element 4:
parasitic oscillation after flyback phase involving mainly the output capacitance of the MOSFET and the magnetization inductance of the transformer</td></tr>
<tr><td>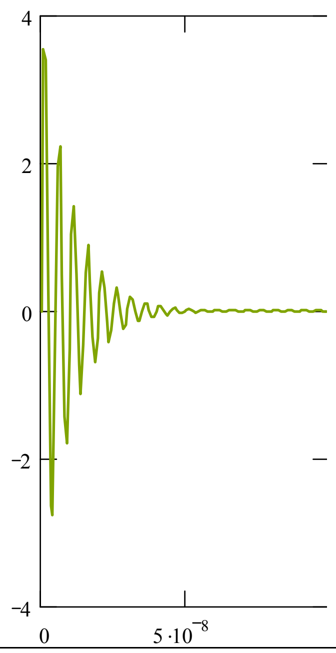
</td><td>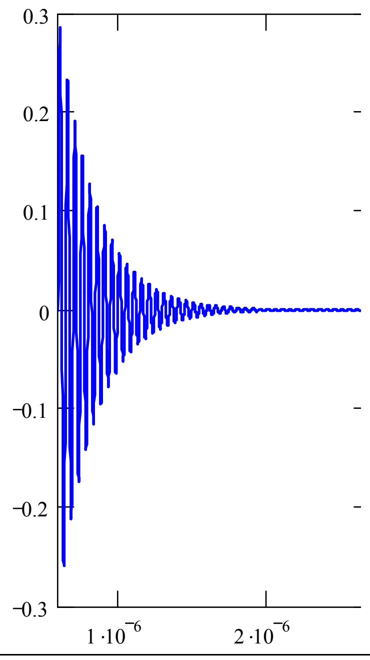
</td><td>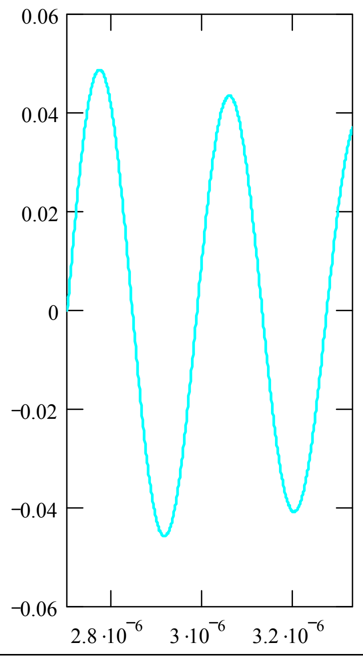
</td></tr>
</table>

Tab. 5 Main elements of the drain current

The spectrum of the whole drain current waveform (Fig. 21) is presented in Fig. 23.

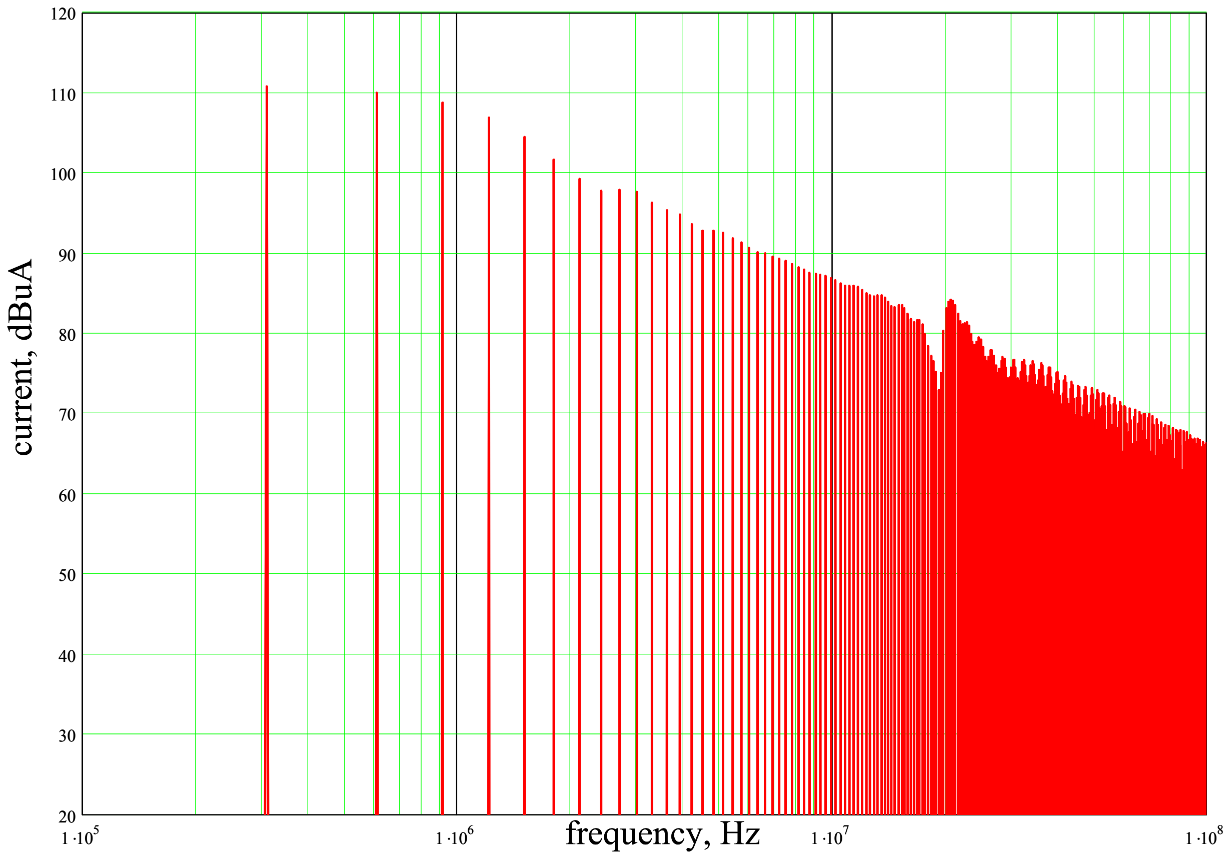

Fig. 23 Spectrum of the drain current (as shown in Fig. 22)

The spectra of the main elements of the drain current can be found in Fig. 25. Fig. 24 is exactly the same as Fig. 22 and has been repeated for better understanding.

As in case of drain-source voltage this method allows to associate the elements of the drain current waveform with its contribution to the whole spectrum. For example, the peak at 20 MHz in the spectrum is caused by the parasitic oscillation due to the output capacitance of the MOSFET and the leakage inductance of the transformer.

This method of separating the waveform in time domain into its main elements helps to find out what part of the spectrum in frequency domain caused by what related physical phenomena. The separation into main elements should be done in respect of reasonable events in the power circuit like on and off slopes, oscillations, clamping, snubbering, reflected voltage, etc.

In this flyback example only the primary switch has been analyzed as active source of electrical noise. There are also others, like secondary side diodes or synchronous rectifier, control IC (especially its gate drive), etc. In order to obtain more complete analysis all these interference sources have to be analyzed.

However, it is impossible to predict the conducted EMI spectrum using this approach due to the fact, that only interference sources are considered. There is no analysis of the spreading paths of the interference in this method.

Nevertheless, the association of harmonics root cause with the respected physical phenomena will reduce the efforts of EMI reduction. The impact of the identified root cause can be reduced not only by filtering, but also by means of influencing the root cause itself.

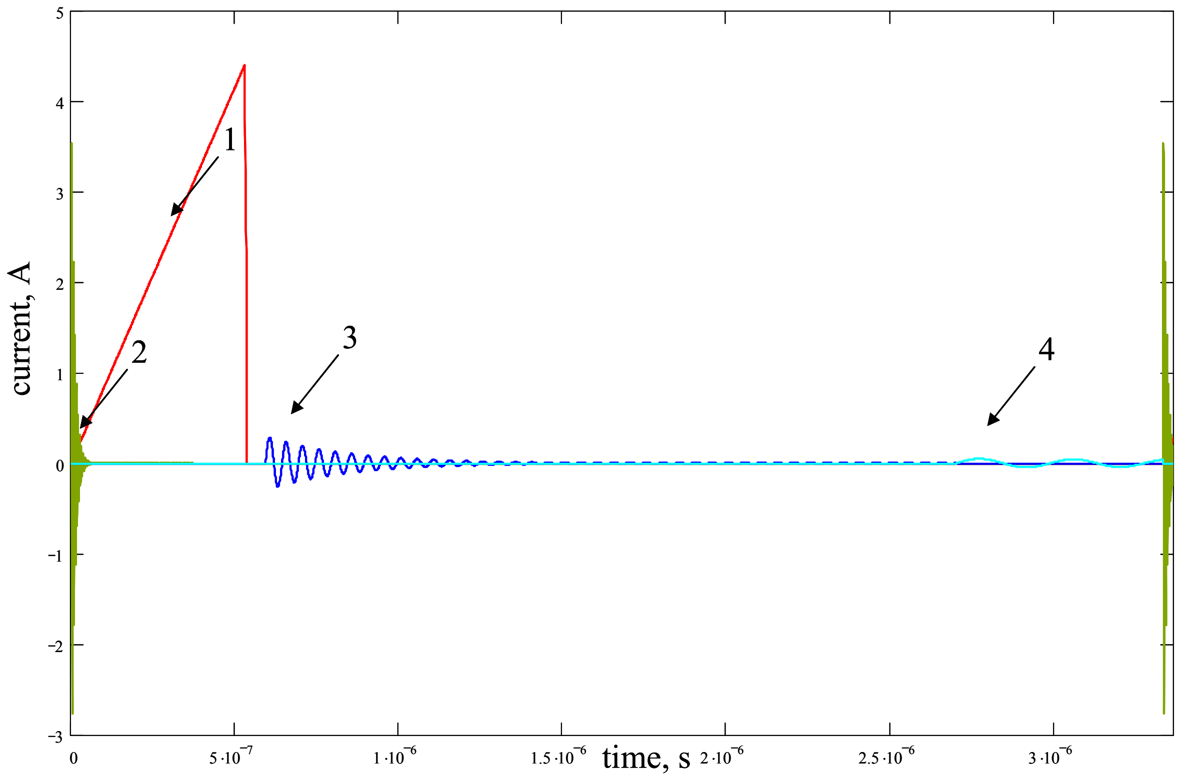

Fig. 24 Main elements of the drain current

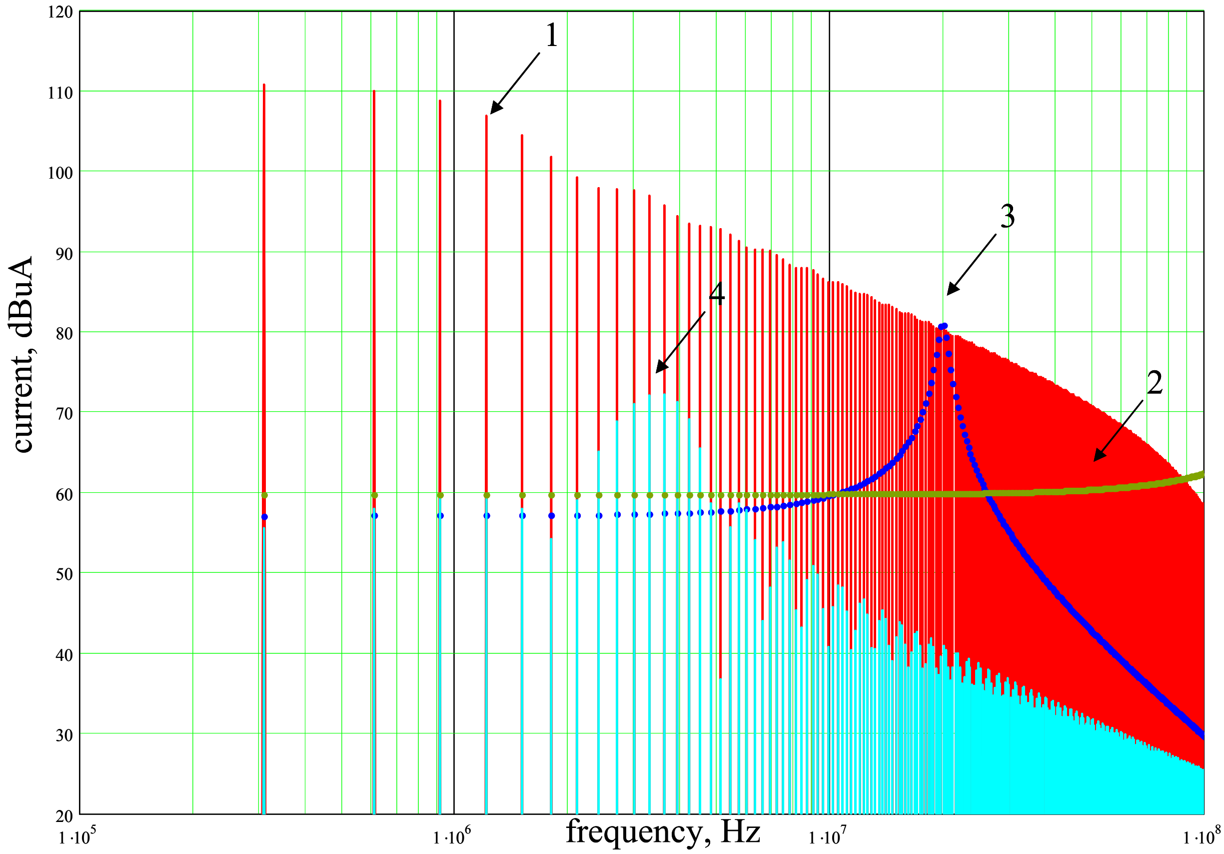

Fig. 25 Spectra of the main elements of the drain current

5.2.2. Operation modes of discontinuous flyback converter

The flyback converter running in discontinuous conduction mode can be operated in hard switching or quasi resonant (or valley switching, or ZVS) mode regarding the primary side switch. The difference between a hard switching and quasi resonant flyback converter is the turn on time point of the primary switch. In a hard switching mode the turning on of the MOSFET is not synchronized with the drain-source voltage value. This type of converters runs mainly in fixed frequency mode.

In a quasi resonant mode the resonant circuit determined by the output capacity of the MOSFET and the inductance of the transformer will be utilized to switch on at lowest possible value of the drain-source voltage. This circuit starts to oscillate at the end of the current flow through the secondary side of the transformer, hence at the end of the flyback phase. The MOSFET will be turned on at the minimum of this oscillation. The quasi resonant approach uses this oscillation to achieve minimum voltage switching during turn on for the MOSFET. This operation mode runs at a variable frequency.

Higher amplitude of the oscillation results in lower drain source voltage level at which the MOSFET turns on correspondingly lower switching losses and higher efficiency of the system.
To achieve high oscillation peaks, the design of the transformer has to be set to high reflected voltage. This increase of the reflected voltage results in a higher drain source voltage blocking MOSFET and longer duty cycles.

Comparison of three different flyback solutions has been made. All of them have been operation at 300 kHz, bus voltage of 400 V, output power of 120 W, output voltage of 16 V. These design included different modes of operation and different values of reflected voltage, resulting in different MOSFET’s voltage ratings:

- Hard switching flyback with CoolMOS™ 600 V, reflected voltage of 100V
- Quasi resonant flyback with CoolMOS™ 600 V, reflected voltage of 100V
- Quasi resonant flyback with CoolMOS™ 800 V, reflected voltage of 390V

The clamping snubber circuit was set to the rated breakdown voltage of the MOSFET (600 V and 800 V respectively).

5.2.3. Flyback in hard switching mode with 600 V MOSFET

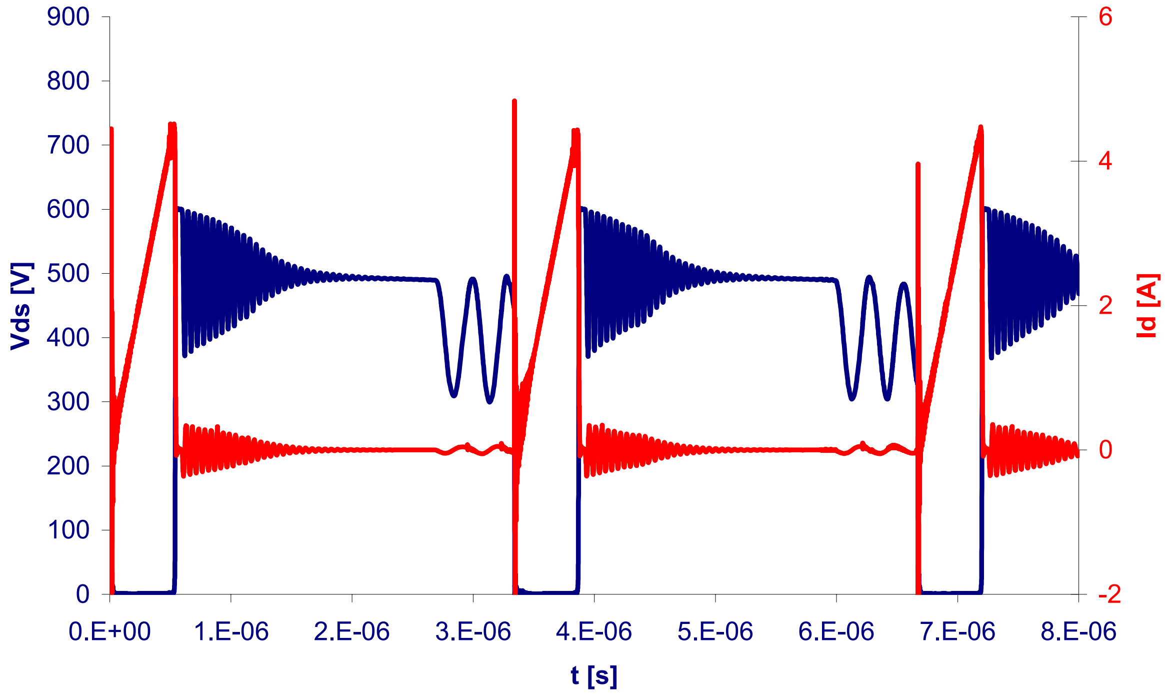

Fig. 26 Drain-source voltage and drain current of hard switching 600V flyback

The hard switching approach (as shown in Fig. 26) doesn't consider the minimum drain-source voltage. The MOSFET will be turned on hard, in this case at a voltage level of 500 V (at time point 3.3 μs). The discharge of circuits' parasitic capacitances leads to a high current spike during turning on.

5.2.4. Flyback in quasi resonant mode with 600 V MOSFET

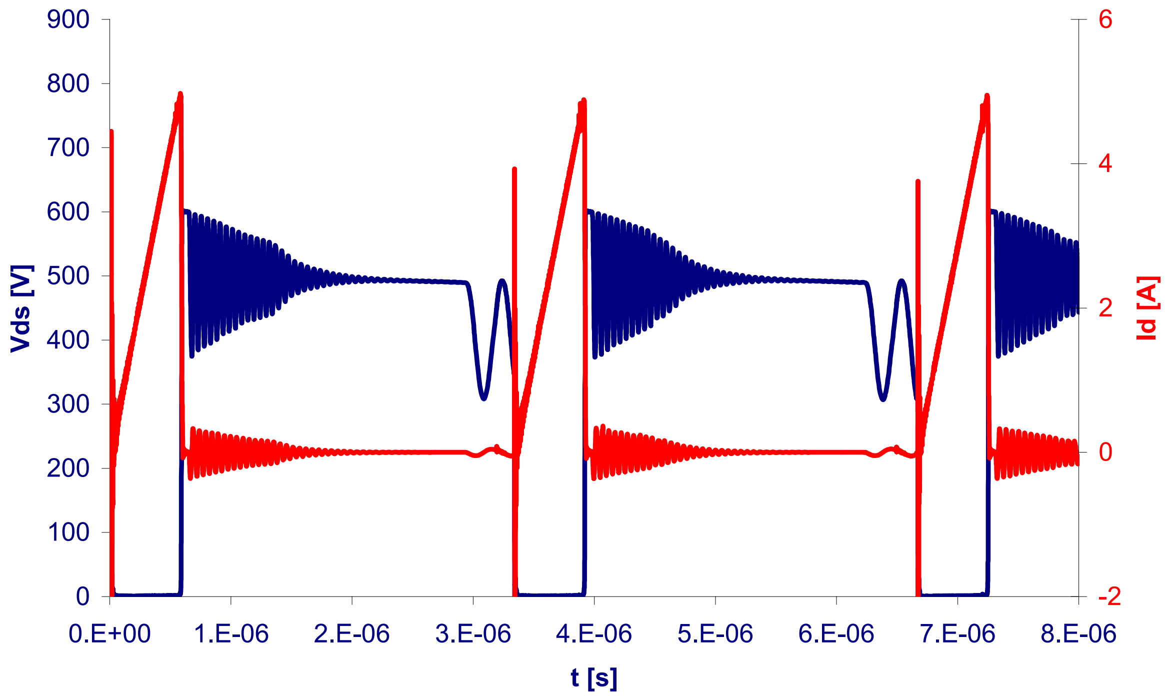

Fig. 27 Drain-source voltage and drain current of quasi resonant 600V flyback

The drain-source voltage (Fig. 27) starts oscillating at the end of the flyback phase and reaching the minimum of 300 V when the MOSFET turns on.
The duty cycle is lower compared to an 800 V solution due to a lower reflected voltage of 100V. Shorter duty cycle for the same output power results in higher peak currents on the primary side.

5.2.5. Flyback in quasi resonant mode with 800 V MOSFET

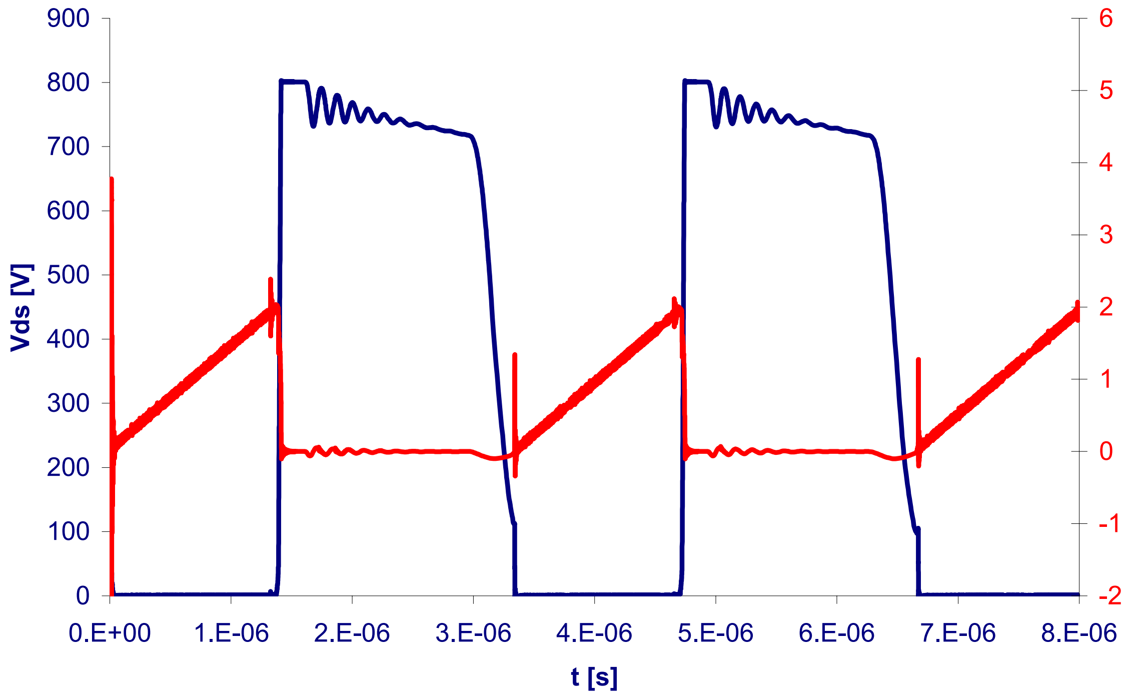

Fig. 28 Drain-source voltage and drain current of quasi resonant 800V flyback

The drain-source voltage (Fig. 28) starts oscillating at the end of the flyback phase and reaching the minimum of 100V when the MOSFET turns on. The turning on current spike is low.
The duty cycle is higher compared to a 600V solution due to a higher reflected voltage of 390V. Longer duty cycle for the same output power results in lower peak currents on the primary side.

5.2.6. Comparison of spectra

The spectra of the drain-source voltages for corresponding flyback design (Fig. 26Fig. 27 and Fig. 28) are shown in Fig. 29.

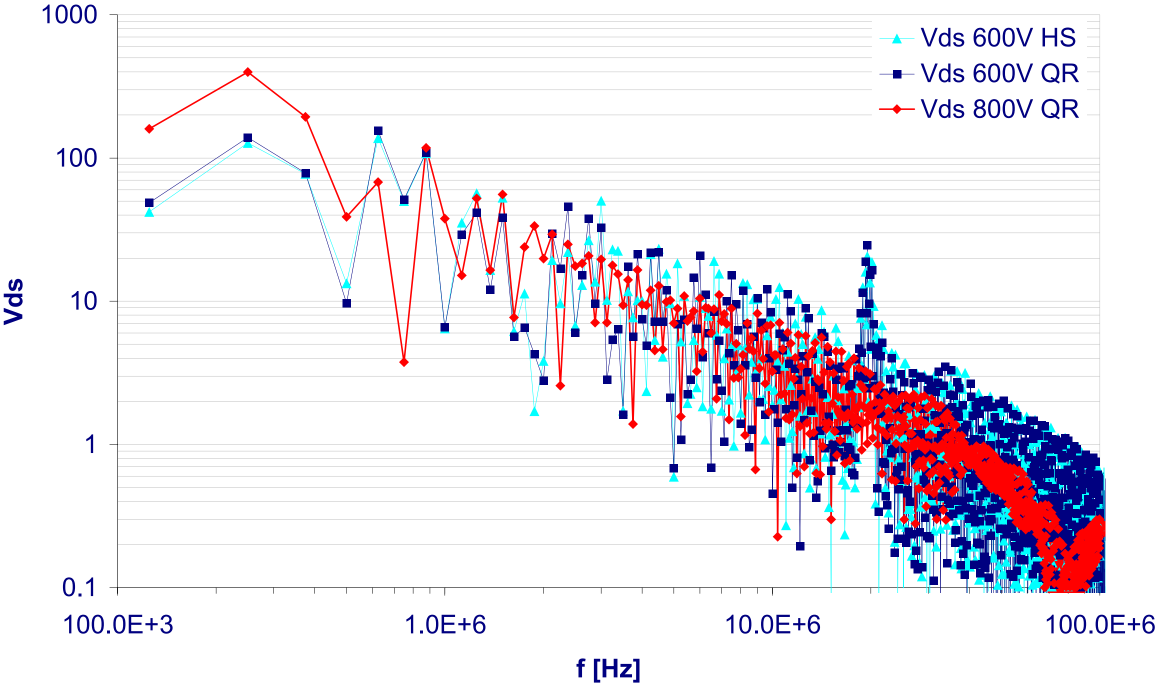

Fig. 29 Spectra of the drain-source voltage (simulated)

As it can be seen the voltage spectrum of the 800V quasi resonant flyback is higher at frequencies below 1 MHz, and is getting lower above 1 MHz compared to both 600V designs. This can be explained by two major differences of the 800V drain-source voltage waveform. First, the clamping voltage during the MOSFETs turning off is 800V, what is higher then of 600V. It leads to higher harmonics amplitudes in lower frequency range. Second, the turn on occurs in voltage minimum due to quasi resonant switching, which results in lower spectrum in higher frequency range.

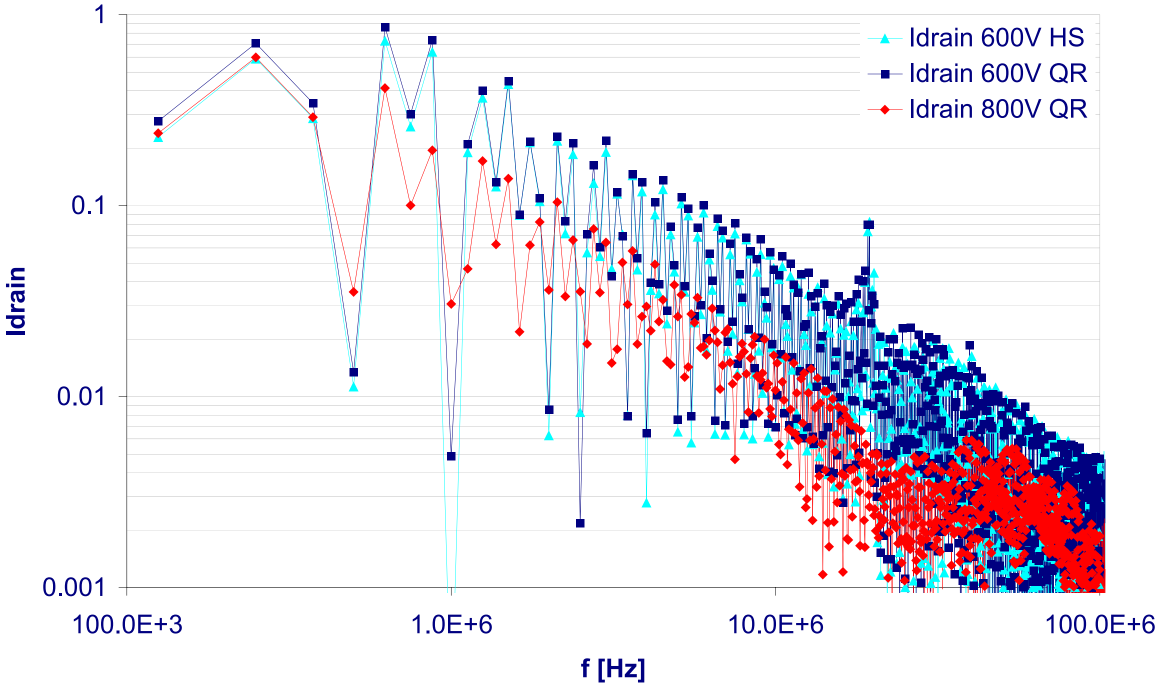

Fig. 30 Spectra of the drain current (simulated)

Due to the fact, that the 800V quasi resonant flyback has lower peak current, its spectrum is significantly lower across almost complete frequency range.

The 800V quasi resonant design with lower current peak and lower drain-source voltage during turning on of the MOSFET demonstrates advantages in conducted EMI spectra regarding the primary side.

6. EMI design aspects

6.1. Circuit layout

The switched current with its steep slopes generates a magnetic field over the power loops where it flows. The loop inside and surrounding will be penetrated by this magnetic field. These loops have to cover as small as possible surface, in order to make the surface penetrated by the magnetic field small. If this is not possible, a low-inductance capacitor of some µF, which is connected parallel to the bulk and close to the switch, may help.

The PCB tracks should be as short and wide as possible, in order to make the effective antenna smaller on the one hand and, on the other hand, to reduce the voltage drop. The wider the track the lower is the length-related resistance and inductance and thus also the static and dynamic voltage drop. This is particularly important for the ground track, since it should have as constant as possible potential for the entire system as point of reference.

A further method, which has to be considered, is the parallel connection of capacitors, in order to reduce their effective parasitic series resistance. The layout for both connectors of the capacitors should be identical. Otherwise the series resistances are not the same and this results a higher current stress of the capacitor with the lower series resistance.

6.2. Transformer

The transformer fulfills not only the task of voltage converter, but also it realizes a potential separation between primary and secondary side. It couples at the same time the two electrically isolated electric circuits by the magnetic induction. Capacitive coupling between primary and secondary side represents a spreading path for interference, e.g. in form of displacement current.
In order to reduce the possible interference between primary and secondary side these capacitive coupling should be reduced. It can be realized by the physical separation of primary and secondary windings, the shielding of the whole transformer as well as the closed shielding of the primary and secondary windings. The shielding inside the transformer should be realized by one foil per side connected to the input or output.

6.3. EMI filter

The measures mentioned above are useful to reduce the EMI; however they are usually not enough to fulfill for required norm regulations. The EMI filters attenuate the electrical noise by creating an absorption and/or a trap circuit. The filters are located at the input and/or output of the system. Fig. 31 demonstrates a typical EMI filter.

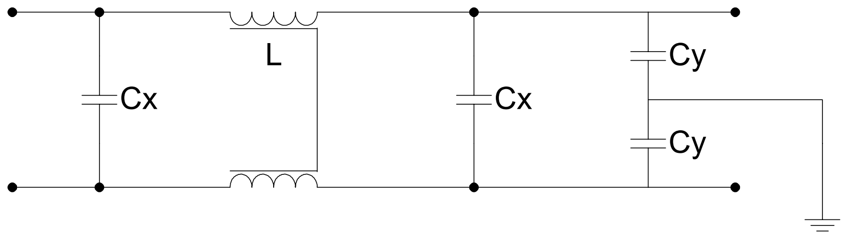

Fig. 31 Typical EMI filter

X-capacitors (C_X) are connected between the connecting lines. This leads a filtering of the differential mode interferences up to some kHz.

In order to reduce interferences above 150 kHz, Y-capacitors (C_Y) between conducting lines and ground, can be used. These have a main effect on the common mode interferences up to some MHz.

A problem of these filters is the influence of the parasitic elements on the real impedance. A real capacitor includes both an inductor and resistor in the form of leads, traces and even ground planes in series with it. Fig. 32 shows the impedance of a 10 nF capacitor with 10 mm long leads. The leads are equivalent to an inductance of L_p=10nH. The capacitor behaves ideally up to frequencies of some MHz. Above the resonant frequency of

$$f_r = \frac{1}{2\pi\sqrt{CL_p}} \approx 16MHz \tag{1}$$

the behavior is defined however exclusively by the inductance of the leads. The resonant frequency of the capacitors determines the maximum effective attenuated frequency (Fig. 32).

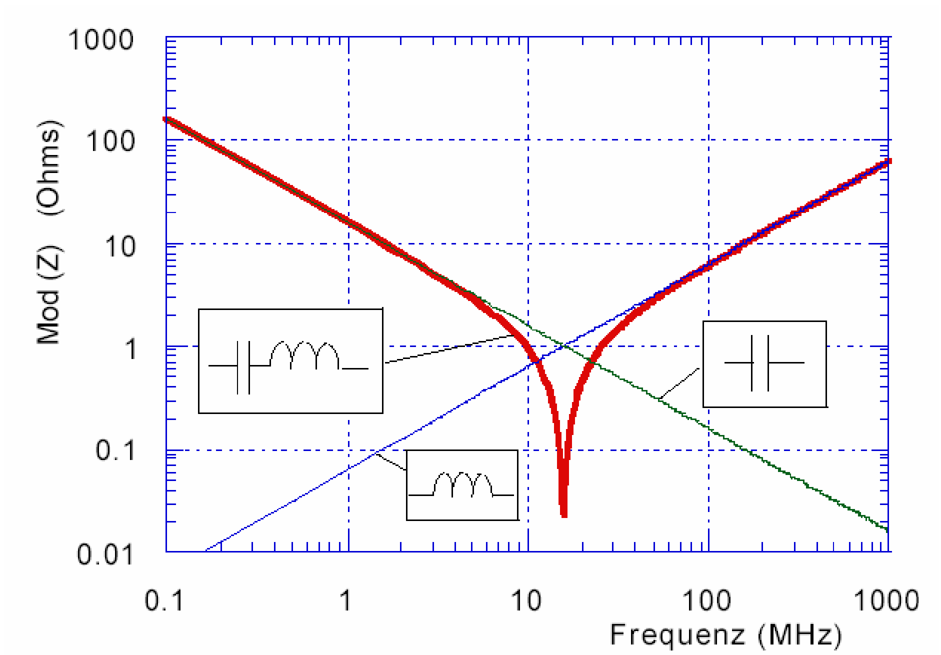

Fig. 32 Impedance of a 10 nF capacitor with 10 mm leads

Ferrites with high insertion loss are applied in a wide frequency range. Common mode interferences are filtered with ferrite sleeves and differential mode interferences with ferrite beads. The ferrite beads have the disadvantage that they absorb also the information signal. In order to prevent this, there are ferrites with special frequency dependent impedance.

Current-compensated chokes are a special form of ferrite sleeves with more than a half turn. They have a large asymmetrical effective inductance, typically some mH, and a very small symmetrical inductance, also leakage inductance. The sum of all currents in this chokes should be zero. A small imbalance will cause the inductor partly going into saturation, which results in a decrease of effective inductance.

7. Summary

This application note presented the basics of Electromagnetic Interference, a short overview of the active regulations in selected regions and showed an example how to measure conducted EMI. Several MOSFET related influence factors on the EMI in SMPS have been investigated experimentally. Different operation modes of a flyback converter have been simulative studied regarding their influence on the electrical noise generation. General design guidelines have been given.

Revision History		
Application Note AN-EMI-01		
Actual Release: V1.1 Date: Jul 2003	Previous Release:	
Page of actual Release	Page of prev. Release	Subjects changed since last release
29		

For questions on technology, delivery and prices please contact the Infineon Technologies Offices in Germany or the Infineon Technologies Companies and Representatives worldwide: see the address list on the last page or our webpage at

http://www.infineon.com

CoolMOS™ and thinQ!™ are trademarks of Infineon Technologies AG.

Edition 2003-07-01
Published by Infineon Technologies AG,
Balanstr. 59,
D-81541 München